The Astrophysical Journal, 547:264–271, 2001 January 20

THE MODIFIED WEIGHTED SLAB TECHNIQUE: MODELS AND RESULTS

Frank C. Jones
Laboratory for High Energy Astrophysics, Code 661, NASA Goddard Space Flight Center, Greenbelt, MD 20771; frank.c.jones@gsfc.nasa.gov
Andrew Lukasiak
Institute for Physical Science and Technology, University of Maryland, College Park, MD 20742; al36@umail.umd.edu
Vladimir Ptuskin
Institute for Terrestrial Magnetism, Ionosphere and Radio Wave Propagation of the Russian Academy of Science (IZMIRAN), Troitsk, Moscow Region 142092, Russia; vptuskin@izmiran.troitsk.ru
and
William Webber
New Mexico State University, Las Cruses, NM 88003
Received 2000 June 26; accepted 2000 September 6

ABSTRACT

In an attempt to understand the source and propagation of Galactic cosmic rays, we have employed the modified weighted slab technique along with recent values of the relevant cross sections to compute primary to secondary ratios including B/C and sub-Fe/Fe for different Galactic propagation models. The models that we have considered are the disk-halo diffusion model, the dynamical halo wind model, the turbulent diffusion model, and a model with minimal reacceleration. The modified weighted slab technique will be briefly discussed and a more detailed description of the models will be given. We will also discuss the impact that the various models have on the problem of anisotropy at high energy and discuss what properties of a particular model bear on this issue.
Subject headings: cosmic rays — diffusion — magnetic fields — shock waves

1. THE APPLICATION OF THE MODIFIED WEIGHTED SLAB TECHNIQUE TO SIMPLIFIED MODELS

The weighted slab technique has long been used in studying the propagation of cosmic rays in the Galaxy from their points of origin to their observation points near the Earth (Davis 1960; Ginzburg & Syrovatskii 1964; Ginzburg & Ptuskin 1976; Lezniak 1979; also see Webber 1997). Several approximations are used in deriving this technique, among them the assumption that energy loss and/or gain is not significant and that the propagation in, and loss from, the Galaxy may be described by a function of energy per nucleon alone. Both of these simplifications are known to be untrue: for low energies, ionization energy loss can be significant and rigidity, or energy per charge, is believed to be the parameter that best describes propagation.

Ptuskin, Jones, & Ormes (1996) showed how the weighted slab technique could be made exact for Galactic propagation models in which energy gains and losses were proportional to the same mass density that determined nuclear fragmentation and time-dependent processes, e.g., radioactive decay, do not play a role. This modification allows for the fact that particles had different (usually higher) energies in the past, and hence different propagation properties, and that propagation is considered to be a function of rigidity, although energy per nucleon is the proper parameter for nuclear fragmentation calculations. Strictly, this technique is rigorous only for models in which the particle propagation parameters are proportional to a single function of energy for each particle species, and hence does not apply to Galactic wind models or turbulent diffusion models. However, most of these models may be closely approximated by simplified homogeneous models in which the mean path length has an exponential distribution with a mean path length that is a particular function of rigidity. It is models of this type and approximation that we discuss in this study. In this paper we present some results of the numerical simulations where the most recent set of spallation cross sections were used.

It should be noted that these models bear a similarity to the well-known leaky-box model in that they all (at least approximately) yield an exponentially decreasing path length distribution. They differ in the manner in which the mean path length varies as a function of energy. The similarity ends here, however; the leaky-box model cannot predict any anisotropy as it considers the cosmic rays to be homogeneously distributed in a "box" of indeterminate size and shape. Furthermore, the only independent parameter in the leaky-box model is the amount of matter traversed or "grammage" which is sufficient for stable nuclei, but radioactive nuclei decay is a function of time, not grammage, so the more realistic models can predict significantly different results for these unstable particles. Since we will be dealing with stable nuclei only in this work, our mathematics will look very much like calculations with the leaky-box model, but it should be remembered that we have significantly different physical models in mind when we do these calculations.

2. CROSS SECTIONS

The cross sections used here now include a completely updated cross-section file for the propagation program. This includes the new primary cross sections in hydrogen targets for C through Ni at 600 MeV nucleon^{-1} as described in Webber et al. (1998a, 1998b), as well as the hydrogen cross sections for essentially all of the secondary nuclei from Li through Mn also at 600 MeV nucleon^{-1} reported in Webber et al. (1998c). The energy dependence of these isotopic cross sections is updated and extended as well, using our earlier charge changing cross sections measured between 300 and 1700 MeV nucleon^{-1} (Webber et al. 1990) and at 15 GeV nucleon^{-1} (Webber et al. 1994) and assuming that the isotopic fractions are generally independent of energy as confirmed by these earlier measurements and those of the Transport Collaboration (Chen et al. 1997).

3. DISK-HALO DIFFUSION MODEL

This propagation model (Ginzburg, Khazan, & Ptuskin 1980; Berezinskii et al. 1990), schematically shown in Figure 1, involves a thin (approximately infinitesimal) disk of matter and an extended, matter-free, halo through which the cosmic rays diffuse with a rigidity-dependent diffusion coefficient, $D(R)$. The distribution function $f(z, p)$ normalized as $N = 4\pi \int dp\, p^2 f$ (where N is the total cosmic-ray number density) obeys the equation

$$-\frac{\partial}{\partial z} D \frac{\partial f}{\partial z} + \frac{\mu v \sigma}{m} \delta(z) f + \frac{1}{p^2} \frac{\partial}{\partial p}\left[p^2 \left(\frac{dp}{dt}\right)_{\rm ion} f\right] = q_0(p)\delta(z) \,. \tag{3.1}$$

Here $D(p, z)$ is the particle diffusion coefficient, $\mu \approx 2.4$ mg cm^{-2} (Ferrière 1998) is the surface mass density of the Galactic disk, $v = \beta c$ is the particle velocity, σ is the total spallation cross section, m is the mean mass of an interstellar atom, $(dp/dt)_{\rm ion} = \mu\delta(z)b_0(p)/m < 0$ describes the ionization energy losses, and $q_0(p)\delta(z)$ is the source term that may include the yield from the fragmentation of heavier nuclei.

We shall assume that diffusion does not depend on position, i.e., $D = D(p)$. There is a cosmic-ray halo boundary at $|z| = H$ where cosmic rays freely exit from the Galaxy.

Integrating equation (3.1) in the vicinity of the Galactic plane $\lim \int_{-\varepsilon}^{\varepsilon} dz(...)$ at $\varepsilon \to 0$, one can find the boundary condition at $z = 0 + \varepsilon$,

$$-2D \frac{\partial f_0}{\partial z} + \frac{\mu v \sigma}{m} f_0 + \frac{1}{p^2}\frac{\partial}{\partial p}\left(p^2 \frac{\mu b_0}{m} f_0\right) = q_0(p) \,, \tag{3.2}$$

where $f_0(p) = f(z = 0, p)$ is the distribution function at the Galactic midplane.

The solution of equation (3.1) at $z \neq 0$ under the boundary condition $f(|z| = H) = 0$ is

$$f = f_0 \frac{H - |z|}{H} \,. \tag{3.3}$$

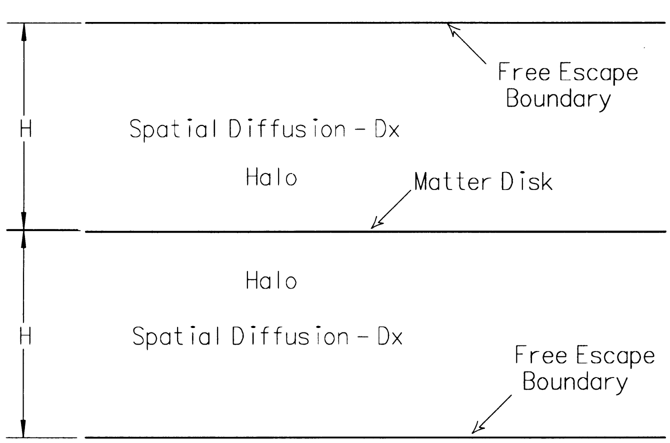

FIG. 1.—Simplified Galactic model with a diffusive halo; Galactic-matter disk is of infinitesimal thickness.

Calculating $-D\partial f_0/\partial z$ from equation (3.3) and substituting it in equation (3.2), one can get the following closed equation for $f_0(p)$:

$$\frac{2Df_0}{\mu v H} + \frac{\sigma}{m} f_0 + \frac{1}{p^2}\frac{\partial}{\partial p}\left(p^2 \frac{b_0}{mv} f_0\right) = \frac{q_0}{\mu v} \,. \tag{3.4}$$

Now we introduce cosmic-ray intensity as a function of kinetic energy per nucleon $I(E_k)dE_k = vf_0(p)p^2 dp$, so that $f_0(p) = I(E_k)A/p^2$ (A is the atomic number). Equation (3.4) gives the following equation for $I(E_k)$

$$\frac{I}{X_{dif}} + \frac{d}{dE_k}\left[\left(\frac{dE_k}{dx}\right)_{\rm ion} I\right] + \frac{\sigma}{m} I = Q \,, \tag{3.5}$$

with the effective escape length for diffusing particles

$$X_{\rm dif} = \frac{\mu v H}{2D} \,, \tag{3.6}$$

and the source term

$$Q = \frac{q_0(p)p^2 A}{\mu v} \,. \tag{3.7}$$

Equation (3.5) is identical to the transport equation for cosmic rays in the so-called leaky-box model, the popular empirical model used in the studies of cosmic-ray propagation. The leaky-box model has the only parameter, the escape length $X_{\rm lb}$, which describes the cosmic-ray propagation, and this parameter is considered as an empirical characteristic determined from cosmic-ray data. The physical meaning of the escape length is that it is equal to the mean thickness of matter traversed by cosmic rays before exit from the Galaxy.

The foregoing consideration confirms the well-known result that the diffusion model with relatively thin Galactic disk (with half-thickness $h \ll H$) and with flat halo (radius of the Galactic disk $R \gg H$) is almost equivalent to the leaky-box model for calculation of the abundance of stable nuclei in cosmic rays (Berezinskii et al. 1990; Ptuskin et al. 1997). The equivalence holds for not very heavy nuclei which have the total cross sections $\sigma \ll (m/X_{\rm dif})(H/h)$. Under this condition, the relation between the parameters of the diffusion model and the equivalent leaky model follows from the equation $X_{\rm dif} = X_{\rm lb}$ that leads to the expression for the diffusion coefficient,

$$D = \mu\beta c H/(2X_{\rm lb}) \,, \tag{3.8}$$

where $\beta = v/c$. In this simplified model the path-length distribution is a decreasing exponential function with a mean path length dependent on energy. Such a dependence is shown in equation (3.9) where the parameters X_0, R_0, and a are determined by the density of the matter disk, the size of the halo, and the spectrum of magnetic turbulence that sets the diffusion coefficient's rigidity dependence, respectively:

$$X_{\rm lb} = \begin{cases} X_0 \beta \text{ g cm}^{-2} & \text{at } R < R_0 \text{ GV} \,, \\ X_0 \beta (R/R_0 \text{ GV})^{-a} \text{ g cm}^{-2} & \text{at } R \geq R_0 \text{ GV} \,, \end{cases} \tag{3.9}$$

where R is the particle rigidity and $\beta = v/c$. This parameterization is valid for particles in the interstellar medium with energies from about 0.4 GeV nucleon^{-1} to 300 GeV nucleon^{-1} where data on secondary nuclei are available. It is worth noting that the same escape length (eq. [3.9]) satisfactorily reproduces both B/C and sub-Fe/Fe ratios (no need for path-length "truncation"). It should be borne in mind, however, that this diffusion model does not predict the sudden change of the mean grammage as a function of energy that is displayed in equation (3.9) at a rigidity of R_0 GV or any other rigidity. This is a strictly (though widely accepted) ad hoc construction that appears to be required by the data. We will see that the models following this one do not require this behavior to be externally imposed.

The physical interpretation of the empirical equation (3.9) for $R > R_0$ GV can be given in the framework of the diffusion model by referring to equation (3.8). The theory of particle resonant scattering and diffusion in the turbulent interstellar medium predicts the scaling of the diffusion coefficient $D_{\rm res} = \kappa \beta R^a$, where the constant κ is determined by the level of hydromagnetic turbulence with the spectrum $W_k\, dk \propto k^{-2+a}\, dk$, $a =$ const. The scattering of particles with Larmor radius r_g is mainly a result of the interaction with inhomogeneities of the scale $1/k \approx r_g$. Since the time to diffuse to the Galactic boundary, and hence the mean grammage traversed, is inversely proportional to the diffusion coefficient, the interpretation is clear. The observations of interstellar turbulence are consistent with the existence of a single power-law spectrum with $0.2 \le a \le 0.6$ at wavenumbers 10^{-20} cm$^{-1} \le k \le 10^{-8}$ cm^{-1} (see Ruzmaikin et al. 1988). The Kolmogorov spectrum, usually considered to be representative of the interstellar spectrum, corresponds to $a = \frac{1}{3}$.

4. GALACTIC WIND MODEL

We consider a one-dimensional galaxy model shown in Figure 2 (the coordinate z is perpendicular to the Galactic plane). Cosmic-ray sources and interstellar gas are concentrated in a thin disk at $z = 0$. (For details of this model see Jokipii 1976; Jones 1979.) The distribution function $f(z, p)$ obeys the equation

$$-\frac{\partial}{\partial z} D \frac{\partial f}{\partial z} + u \frac{\partial f}{\partial z} - \frac{du}{dz}\frac{p}{3}\frac{\partial f}{\partial p} + \frac{\mu v \sigma}{m}\,\delta(z) f + \frac{1}{p^2}\frac{\partial}{\partial p}\left[p^2 \left(\frac{dp}{dt}\right)_{\rm ion} f\right] = q_0(p)\delta(z)\,, \tag{4.1}$$

where u is the wind-convection velocity.

We shall assume that the wind velocity u is constant and directed outward from the Galactic plane. There is a cosmic-ray halo boundary at $|z| = H$ where cosmic rays freely exit from the Galaxy. Using the same prodecure as in

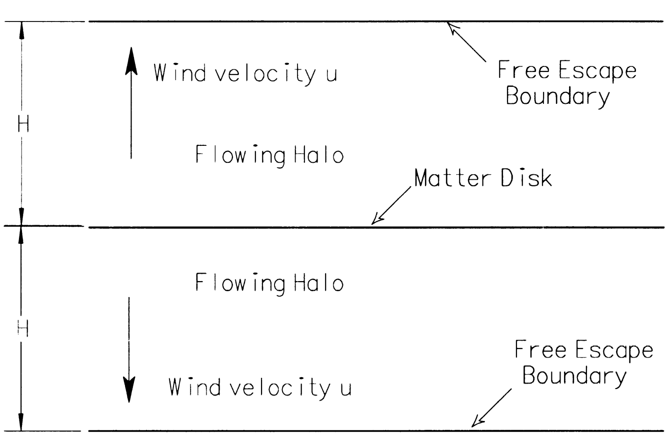

FIG. 2.—Simplified Galactic model with a halo wind; Galactic-matter disk is of infinitesimal thickness.

§ 3, we integrate equation (4.1) in the vicinity of the Galactic plane ($\lim_{\varepsilon\to 0} \int_{-\varepsilon}^{\varepsilon} dz ...$), one can find the boundary condition at $z = 0 + \varepsilon$:

$$-2D \frac{\partial f_0}{\partial z} - \frac{2up}{3}\frac{\partial f_0}{\partial p} + \frac{\mu v \sigma}{m} f_0 + \frac{1}{p^2}\frac{\partial}{\partial p}\left(p^2 \frac{\mu b_0}{m} f_0\right) = q_0(p)\,, \tag{4.2}$$

where $f_0(p) = f(z = 0, p)$ is the distribution function at the Galactic midplane.

The solution of equation (4.1) at $z \ne 0$ under the boundary condition $f(|z| = H) = 0$ is

$$f = f_0 \frac{1 - \exp\left[-u(H - |z|y)/D\right]}{1 - \exp\left(-uH/D\right)}\,. \tag{4.3}$$

Calculating $-D\partial f_0/\partial z$ from equation (4.3) and substituting it in equation (4.2), one can get the following equation for $f_0(p)$:

$$\frac{2uf_0}{\mu v[\exp(uH/D) - 1]} - \frac{2u}{3\mu v} p \frac{\partial f_0}{\partial p} + \frac{\sigma}{m} \times f_0 + \frac{1}{p^2}\frac{\partial}{\partial p}\left(p^2 \frac{b_0}{mv} f_0\right) = \frac{q_0}{\mu v}\,. \tag{4.4}$$

Equation (4.4) gives the following equation for the cosmic-ray intensity:$I(E_k)$

$$\frac{I}{X_w} + \frac{d}{dE_k}\left\{\left[\left(\frac{dE_k}{dx}\right)_{\rm ad} + \left(\frac{dE_k}{dx}\right)_{\rm ion}\right] I\right\} + \frac{\sigma}{m} I = \frac{q_0(p) p^2 A}{\mu v} \tag{4.5}$$

with the effective escape length

$$X_w = \frac{\mu v}{2u}\left[1 - \exp\left(\frac{-uH}{D}\right)\right], \tag{4.6}$$

and the adiabatic energy loss rate per g cm^{-2}

$$\left(\frac{dE_k}{dx}\right)_{\rm ad} = -\frac{2u}{3\mu c}\sqrt{E_k(E_k + 2E_0)}\,. \tag{4.7}$$

At this point we have arrived at an equation that is essentially the same as for the thin disk-halo model in the sense that the path-length distribution will be an exponential with the mean path length given by X_w. We may therefore apply the modified weighted slab technique to solve the equations.

As before, the asymptotic scaling of X_w in this case is

$$X_w = \frac{\mu v}{2u} \propto v \text{ at small rigidities (when } uH/D \gg 1)\,, \tag{4.8}$$

$$X_w = \frac{\mu v H}{2D} \propto R^{-a} \text{ at large rigidities (when } uH/D \ll 1)\,. \tag{4.9}$$

It should be noted that here the flattening of the curve of mean grammage versus energy at low energy arises naturally from the model and does not need to be inserted by hand.

Equation (4.6) may be presented in the following form useful to fit the observations:

$$X_w = \beta X_0 \left\{ 1 - \exp\left[-\frac{1}{\beta (R/R_0)^a} \right] \right\} . \quad (4.10)$$

Here $X_0 = (\mu c)/(2u)$, and $R_0 = (uH/\kappa_0)^{1/a}$. The adiabatic energy loss term, equation (4.7) in these notations, reads

$$\left(\frac{dE_k}{dx} \right)_{\rm ad} = -\frac{1}{3X_0} \sqrt{E_k(E_k + 2E_0)} . \quad (4.11)$$

It is worth noting that here we consider only a simple model with constant wind velocity. In more realistic models the wind velocity depends on the distance from the Galactic plane, e.g., in a self-consistent model of a cosmic-ray driven Galactic wind (Ptuskin et al. 1997).

5. TURBULENT DIFFUSION

In this model there is no regular convective (wind) transport; rather, the flow is turbulent and the transport of the particles is more random. In fact the convection in this flow is of the same nature as diffusion with the diffusive properties determined by the random flow (see Fig. 3). Equation (4.1) becomes

$$-\frac{\partial}{\partial z} D \frac{\partial f}{\partial z} + \frac{\mu v \sigma}{m} \delta(z) f + \frac{1}{p^2} \frac{\partial}{\partial p} \left[p^2 \left(\frac{dp}{dt} \right)_{\rm ion} f \right] = q_0(p) \delta(z) . \quad (5.1)$$

The equation for $I(E_k)$ is the following

$$\frac{I}{X_{\rm dif}} + \frac{d}{dE_k} \left[\left(\frac{dE_k}{dx} \right)_{\rm ion} I \right] + \frac{\sigma}{m} I = \frac{q_0(p) p^2 A}{\mu v} , \quad (5.2)$$

where

$$X_{\rm dif} = \frac{\mu v H}{2D} . \quad (5.3)$$

We assume now that cosmic-ray diffusion is provided simultaneously by turbulent diffusion with the diffusion coefficient D_t that does not depend on particle energy (may be estimated as $D_t = u_t L_t/3$, where u_t and L_t are the characteristic random velocity and correlation scale of large-scale turbulent motions of the interstellar gas) and by resonant diffusion with the diffusion coefficient $D_{\rm res} = \beta \kappa_0 R^a$ (here $\kappa_0 = {\rm const}$, $a = {\rm const}$) provided by the scattering on hydromagnetic turbulence as was discussed in the previous section. The total diffusion coefficient which appears in equation (5.3) is equal to

$$D = D_t + D_{\rm res} . \quad (5.4)$$

Equation (5.3) may be presented in the following form that is useful to fit the observations:

$$X_{\rm dif} = \frac{\beta X_0}{1 + \beta (R/R_0)^a} . \quad (5.5)$$

Here $X_0 = (\mu c H)/(2D_t)$, and $R_0 = (D_t/\kappa_0)^{1/a}$.

We note again that the flattening of the mean grammage versus energy curve for low rigidities, as in the previous wind model, arises naturally from the physical picture. Actually the reason is the same in both models; below a particular rigidity kinetic diffusion becomes slower than the convective transport in removing particles from the galaxy and the particles, residence time becomes independent of rigidity or energy.

6. STOCHASTIC REACCELERATION

This model (Seo & Ptuskin 1994) assumes no convective or wind motion in the system (see Fig. 4). As before, the spatial diffusion is provided by scattering on random hydromagnetic waves with a spectrum that results in $D \propto vR^a$. For a Kolmogorov spectrum of turbulence, $a = \frac{1}{3}$; but we shall consider the value of a as a free parameter, in the same way as in the models discussed above. This determines the behavior of the escape length $X_e = X_0 R^{-a}$ (see eq. [4.9]) at all energies. So far this does not differ from the diffusion model, but here we consider the fact that the turbulence is not static; rather, the magnetic fluctuations move with the Alfvén velocity, producing a diffusion in momentum as well as in space. Stochastic acceleration with a diffusion coefficient in momentum $K \sim p^2 v_{\rm A}^2/D$ ($v_{\rm A}$ is the Alfvén velocity) essentially modifies the spectra of primaries and secondaries below about 10 GeV nucleon^{-1} and can produce the characteristic peak in B/C ratio at few GV. The acceleration becomes inefficient at high energies, and the model is reduced to a simple diffusion model without reacceleration and with the escape length $X_e = X_0 R^{-a}$ at $E > 20$–30 GeV nucleon^{-1}.

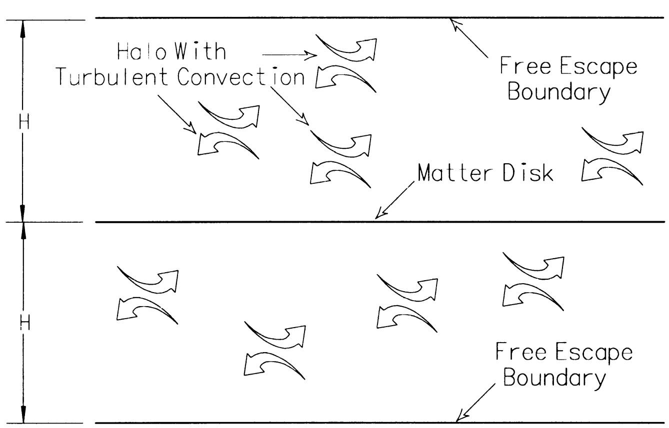

FIG. 3.—Turbulent diffusion model. Halo is diffusive with two types of diffusion.

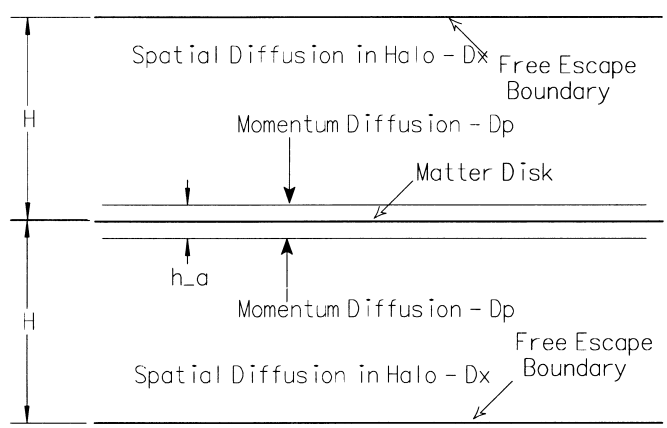

FIG. 4.—Reacceleration model. Halo is diffusive in momentum as well as space.

We use the same notations as Seo & Ptuskin (1994) and use their equation (12) for the calculations:

$$\frac{I}{X_e} + \frac{\sigma}{m} I + \frac{d}{dE}\left[\left(\frac{dE}{dx}\right)_{\rm ion} I\right] + \alpha\left\{\left[\frac{A}{Z}\frac{(E_k + E_0)}{\beta}\frac{dX_e}{dR} + X_e\right]I - \frac{A}{2Z}\beta(E_k + E_0)^2\frac{dX_e}{dR}\frac{dI}{dE} - \frac{\beta^2}{2}(E_k + E_0)^2 X_e \frac{d^2 I}{dE^2}\right\} = \frac{q_0(p)p^2 A}{\mu v} . \quad (6.1)$$

Here the parameter α, which is defined as

$$\alpha = \frac{32}{3a(4 - a^2)(4 - a)}\frac{h_a}{H}\left(\frac{v_a}{\mu c}\right)^2 \quad (6.2)$$

[its dimension is (g cm^{-2})$^{-2}$], determines the efficiency of reacceleration; h_a is the height of the reacceleration region. In this work we have taken $h_a/H = \frac{1}{3}$.

The parameters we have to find from fitting the data are X_0, α, and a, since we will not prescribe the spectrum of the interstellar turbulence.

7. FITS TO DATA

We fitted the four models discussed above to a collection of data compiled by Stephens & Streitmatter (1998) for the B/C and for the sub-Fe/Fe ratios. We determined which parameters best fit (in the weighted least-squares sense) both ratios simultaneously for each model. The parameters found for each model are given in Table 1. It should be noted that because considerable computing is required for each set of parameter values, the search in parameter space was not automated. It was performed by hand and thus we can not guarantee that the fits that we have found are rigorously least-squares fits; they are simply the smallest values we could find in our searches.

These parameters imply physical quantities for the different models given in Table 2. Notice that certain parameters are meaningful for specific models only, not all models in general.

In the turbulent diffusion model the turbulent diffusion coefficient can be estimated as $D_t = u_t L/3$, where u_t is the characteristic velocity and L is the characteristic scale of the turbulent motions. Since we would not expect the magnitude of the velocity u_t to exceed 100 km s^{-1}, that leads to the very large value of $L \geq 0.76H$. Thus this model of cosmic-ray transport requires a value of D_t that is difficult to reconcile with acceptable values of parameters of the interstellar turbulence.

These fits are displayed with the data in Figures 5 and 6.

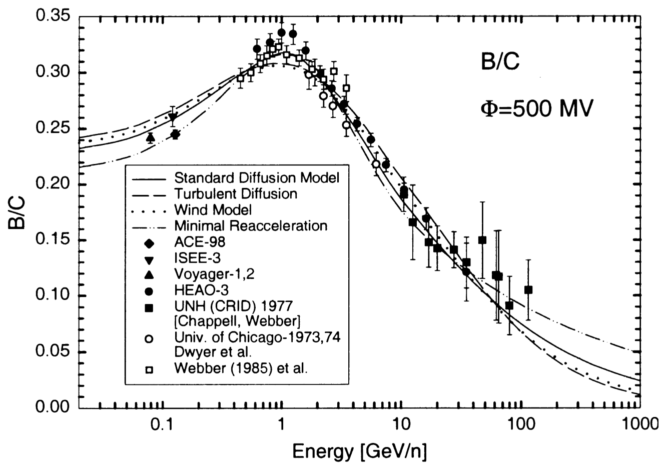

FIG. 5.—Least-squares fit to observed B/C ratios, in four propagation models: turbulent diffusion (*dashed lines*), wind (*dotted lines*), reacceleration (*dash-dotted lines*), and the disk-halo diffusion model with the diffusion coefficient given by eq. (3.8) (*solid lines*). Φ is the force-field approximation solar modulation parameter. Data are from a comprehensive compilation by Stephens & Streitmatter (1998).

TABLE 1

BEST-FIT PARAMETERS FOR FITTING SECONDARY/PRIMARY RATIOS FOR THE MODELS CONSIDERED

	FITTED PARAMETERS			
MODEL	X_0 (g cm^{-2})	R_0 (GV)	a	χ^2 (Normalized)
Disk-halo diffusion	11.8	4.9	0.54	1.3
Wind	12.5	11.8	0.74	1.5
Turbulent diffusion	14.5	15.0	0.85	1.8
Stochastic reacceleration	9.4	$\alpha = 2.6 \times 10^{-3}$	0.30	1.8

NOTE.—For minimal reacceleration there is no R_0 parameter; rather, the strength of acceleration is given by the dimensionless parameter α.

TABLE 2

PHYSICAL PARAMETERS IMPLIED BY THE FIT PARAMETERS OF TABLE 1

	PHYSICAL PARAMETERS			
MODEL	$D_{\rm res}$ (cm^2 s^{-1})	D_t (cm^2 s^{-1})	u (km s^{-1})	V_a (km s^{-1})
Disk-halo diffusion	$2.0 \times 10^{28}\beta$	...	...	...
Wind	$7.2 \times 10^{27}\beta$	...	29	...
Turbulent diffusion	$3.8 \times 10^{27}\beta$	3.8×10^{28}	...	...
Stochastic reacceleration	$5.9 \times 10^{28}\beta$	...	...	40

NOTE.—The values of $D_{\rm res}$ should be multiplied by R^a with R in GV and a taken from Table 1.

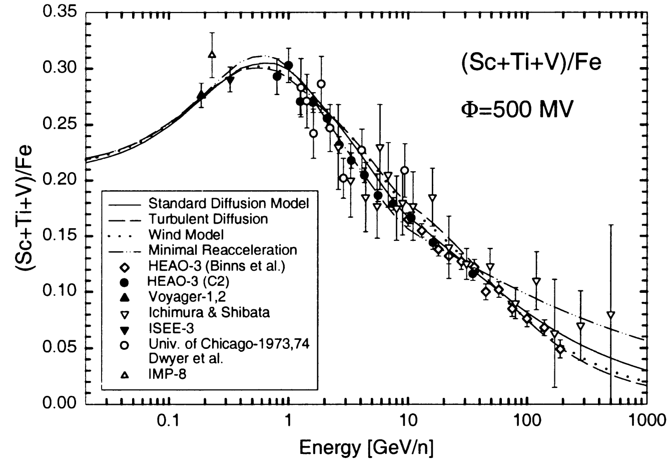

FIG. 6.—Least-squares fit to observed sub-Fe/Fe ratios, in four propagation models: turbulent diffusion (*dashed lines*), wind (*dotted lines*), reacceleration (*dash-dotted lines*), and the disk-halo diffusion model with the diffusion coefficient given by eq. (3.8) (*solid lines*). Φ is the force-field approximation solar modulation parameter. Data are from a comprehensive compilation by Stephens & Streitmatter (1998).

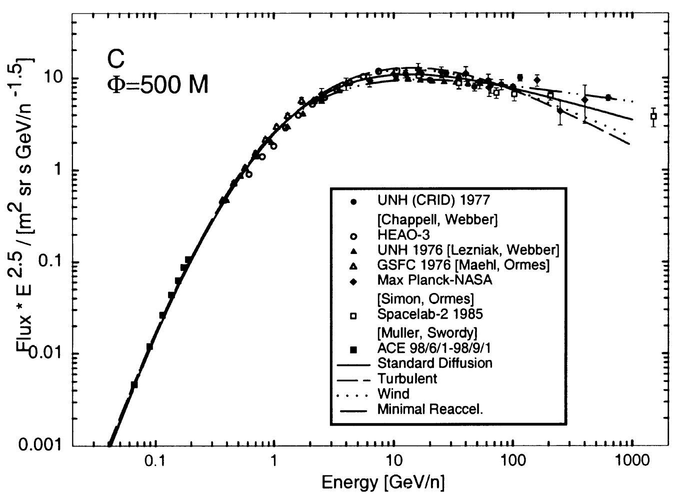

FIG. 7.—Least-squares fit to the C spectrum in the same propagation models as indicated in Figs. 5 and 6.

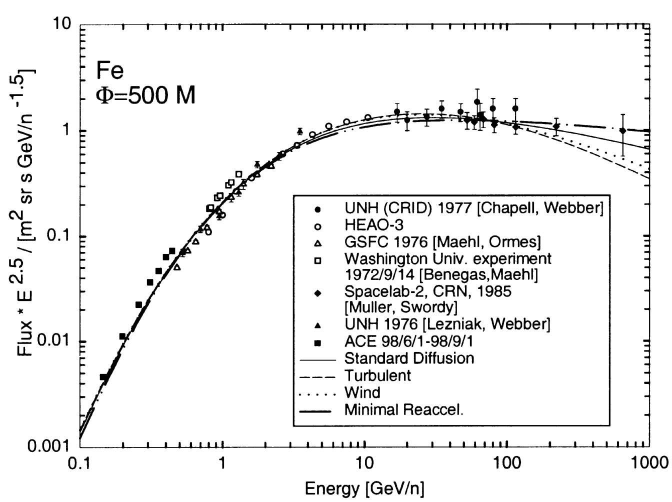

FIG. 8.—Least-squares fit to the Fe spectrum in the same propagation models as indicated in Figs. 5 and 6.

After determining the best-fit parameters, we then used them to propagate primary spectra for C, O, and Fe as discussed in § 8. If one compares Figures 5 and 6 with Figures 7 and 8 (see § 8), one can see how much more sensitive secondary-to-primary ratios are to the propagation model than are simple primary spectra. Although the models were all chosen to fit the same secondary-to-primary data, one can still see significant differences in the model curves, whereas in the plots of carbon and iron the model curves are quite hard to distinguish from one another.

8. SOURCE SPECTRUM

Using the above-determined propagation models, we tested different source spectra to fit observed spectra of primary nuclei C, Fe at energies 0.5–100 GeV nucleon^{-1}. The best fit for the disk-halo diffusion, wind, and turbulent diffusion model is provided by the source spectrum $Q \propto R^{-2.35}$; for the minimal reacceleration model the best fit was obtained with $Q \propto R^{-2.40}/[1-(R/2)^{-2}]^{1/2}$. Figures 7 and 8 show how the different propagation models fit the observations assuming these source spectra. One can expect that asymptotically at very high energies, $E > 100$ GeV nucleon^{-1}, the relation $\gamma = \gamma_s + a$, where $\gamma(\gamma_s)$ is the exponent of the observed (source) differential spectrum $I(E) \propto E^{-\gamma}$, is fulfilled. It is of interest that three of the four models were well fitted with a source spectrum that was a simple power law in rigidity. Only the minimal reacceleration model required a modification at low (nonrelativistic) energies. A similar behavior was found by Heinbach & Simon (1995) in their investigation of a reacceleration model.

It should be noted, however, that the fits were for energies up to $\sim$100 GeV nucleon^{-1}. For much higher energy the fits for models other than the minimal reacceleration model would predict observed spectra much steeper than is observed, unless one assumes a significantly harder source spectrum than the one employed here.

9. ANISOTROPY CONSTRAINT

The observed Galactic cosmic rays are highly isotropic. The amplitude of the first angular harmonic of the cosmic-ray distribution in the interstellar medium near the solar system is approximately equal to $\delta = (0.5\text{–}1.0) \times 10^{-3}$ at energies 10^{12}–10^{14} eV (Nagashima et al. 1989; Cutler & Groom 1991; Aglietta et al. 1993; Alekseenko et al. 1993). The anisotropy is almost energy independent, but a slow increase with energy or even irregular behavior at energies close to 10^{14} eV are not excluded.

Possible interpretation of these observations is based on a contribution of local cosmic-ray sources (Dorman et al. 1984). Supernovae and their remnants are assumed to be the instantaneous point sources. The cosmic-ray density is determined by the total contribution from numerous sources (SN outbursts occur about each 30 yr, whereas the cosmic-ray confinement time in the Galaxy exceeds 10^7 yr). However, the anisotropy may be defined by an individual nearby source. If the diffusion coefficient $D(E)$ increases with energy, the contribution of an individual outburst at distance r gives rise to an anisotropy which depends non-monotonically on energy. A source's contribution to the anisotropy amplitude reaches its maximum when $t \sim r^2/D$, where t is the age of instantaneous source. Analysis of the list of supernova remnants and pulsars indicates that Geminga, Vela, Lupus Loop, Loop III, and some others may prove to be the sources sustaining the anisotropy observed at 10^{12}–10^{14} eV.

One has to check the compatibility of the propagation models discussed in the previous sections with the data on cosmic-ray anisotropy. Each of these models assumes a specific energy dependence of cosmic-ray leakage from the Galaxy. It might result in an anisotropy which exceeds the observational limit. The effect of the solar wind masks the anisotropy of Galactic cosmic rays at energies less than about 10^{12} eV for an observer at the Earth. Below we assume that the dependence of cosmic-ray diffusion on energy determined from the observations of secondary-to-primary ratios in cosmic rays at energies up to about 10^{11} eV can be extrapolated to energies of 10^{12}–10^{14} eV. This simplifying assumption is based on the observation that there is not any drastic change in the total cosmic-ray energy spectrum in the energy range 10^{10}–10^{14} eV that would be indicative of change in the energy dependence of cosmic-ray transport.

The equation for the amplitude of cosmic-ray anisotropy perpendicular to the Galactic plane is the following (see, e.g., Berezinskii et al. 1990):

$$\delta = -\frac{3}{vf}\left(D\frac{\partial f}{\partial z} + u\frac{p}{3}\frac{\partial f}{\partial p}\right), \tag{9.1}$$

which includes both the diffusion and convection fluxes of cosmic rays.

It is easy to show that diffusion dominates over convection at high enough energies $E > 100$ GeV and that effects of ionization energy losses and reacceleration are not essential at these energies in the models we discuss here. Notice also that cosmic-ray anisotropy is mainly determined by the most abundant proton component of cosmic rays that is subject to insignificant effect of nuclear interaction with the interstellar gas. In these conditions, the second term in parentheses in equation (9.1) can be omitted, and the cosmic-ray transport equation can be presented in a simple form as

$$-\frac{\partial}{\partial z}D\frac{\partial f}{\partial z} = q_0(p)\delta(z)\ . \tag{9.2}$$

Now it is easy to show that the anisotropy for an observer just above the δ-plane with cosmic-ray sources is approximately equal to

$$\delta_0 \approx \frac{3q_0(p)}{2vf_0} \approx \frac{3\mu}{2X}\ , \tag{9.3}$$

in all diffusion models . Here X is the escape length which obeys the equation $X \approx \mu\beta cH/(2D)$ at high particle energies.

Cosmic-ray anisotropy inside the source region is smaller than δ_0. For cosmic-ray sources uniformly distributed through the disk with a total thickness $2h$, the anisotropy at distance z from the central Galactic plane is estimated as $\delta_z \approx \delta_0 z/h$ at $|z| < h$ (Ptuskin 1997) . With parameters found in the previous sections and extrapolated to energy 10^{14} eV and with assumption that $z/h = 0.1$ ($z = 20$ pc, $h = 200$ pc), we have the following expected values of the anisotropy $\delta_z(10^{14}$ eV), which is a result of the streaming of cosmic rays perpendicular to the Galactic plane: 7×10^{-3} in the basic diffusion model, 4×10^{-2} in the model with turbulent diffusion, 2×10^{-2} in the Galactic wind model, and 1×10^{-3} in the minimal reacceleration model. These values are uncomfortably large, even for the minimal reacceleration model.

Of course, the models of the galaxy that we have employed here are highly simplified, primarily in the high degree of symmetry and smoothness that they exhibit. This means that the anisotropies that we have calculated are most likely lower limits to those that would be obtained from more complex models. It is always possible to construct models with the solar system in a rather favored position of symmetry that would produce a smaller value of the anisotropy, but such models, lacking any particular knowledge of their reality, are a priori unlikely.

10. CONCLUSION

The objective of the present work was to investigate several models of cosmic-ray propagation and nuclear fragmentation in the interstellar medium using the most recent set of spallation cross sections and employing the modified weighted slab method, which allows us to obtain exact solutions. It is clear from a comparison of Figures 5 and 6 on the one hand and Figures 7 and 8 on the other that the secondary-to-primary ratio is a much more sensitive function of the propagation model (and relatively insensitive to the assumed source spectrum) than is the relation of an observed spectrum to the source spectrum. It is for just this reason that we used this ratio to test our various models before subsequently deducing primary spectra. The standard flat-halo diffusion model, the models with turbulent diffusion, the model with constant wind velocity, and the diffusion model with reacceleration were tested. For each model we then picked the parameter set that best fitted the data. The primary spectra were then calculated for each model using these parameters. All these models are able to explain the decrease of secondary/primary ratios at energies below a few GeV nucleon^{-1}. The turbulent diffusion and the wind transport work simultaneously with resonant diffusion. The last process dominates in cosmic-ray transport at high energies. In order to reproduce a sufficiently sharp bend in the secondary/primary ratio in these models, the diffusion must have a strong dependence on rigidity $D_{res} \propto \beta R^a$, where $a = 0.74$–0.85, at least at low energy ($E < 30$ GeV nucleon^{-1}). However, this could lead to a problem. The extrapolation of such strong rigidity dependence of diffusion to energies 10^3–10^5 GeV produces anisotropies that are at strong variance with the observed anisotropy at these energies.

The disk-halo diffusion model has less severe problems with the explanation of observed small anisotropy than the models with turbulent diffusion and wind. Also, the scaling of diffusion coefficient on rigidity $D_{res} \propto \beta R^{0.54}$ at large rigidities $R > 4.9$ GV in this model is probably not in contradiction with the observations of interstellar turbulence. At the same time, the sharp changeover of the diffusion to the regime $D =$ const at rigidities $R < 4.9$ GV cannot be naturally explained by the kinetic theory of particle scattering in random magnetic fields. The ad hoc elucidation of the observed peak in the secondary-to-primary ratios makes the model implausible.

The reacceleration model is favored as regards its natural description of the energy dependence of particle transport in the Galaxy with a close to Kolmogorov spectrum of turbulence, since the scaling $D_{res} \propto \beta R^{0.3}$ at all rigidities is assumed in this case. The structure of the peak in the secondary-to-primary ratios is reproduced in this model.

The model with reacceleration has no problems accounting for low anisotropy of cosmic rays. However, the predicted weak energy dependence of secondary-to-primary ratios at energies $\gtrsim 20$ GeV nucleon^{-1} is not in agreement with the high-energy *HEAO 3* data by Binns et al. (1981) on the sub-Fe/Fe ratio (see Fig. 6).

The source spectra for primary nuclei derived in all propagation models are close to $R^{-2.3}$ to $R^{-2.4}$ that is uncomfortably steep compared with the predictions of supernova shock acceleration models (Baring et al. 1999; Berezhko & Ellison 1999). Strictly speaking, this refers only to the limited energy range up to about 30 GeV nucleon^{-1}, where statistically accurate data on secondary and primary nuclei are available. Even if one does not assume that a single power-law source spectrum continues to much higher energies, the soft dependency of diffusion on energy in the reacceleration model implies a steep source spectrum close to $R^{-2.4}$ to fit the observed spectrum of primaries close to $R^{-2.75}$. This problem may be not so pressing for the disk-halo diffusion model.

It is interesting to note that current information from high-energy gamma-ray observations may favor such steeper source spectra. While the EGRET measurements (Sturmer & Dermer 1995; Esposito et al. 1996) of gamma rays from certain supernova remnants indicate a flat ($\propto E^{-2.1}$) spectrum at about 100 MeV, however, ground-based detectors place upper limits at energies up to 100 TeV (see Hillas 1996 for a review of these observations) that indicate that the spectrum must have a spectral index of 2.4 or greater.

It is clear that measurements of secondary-to-primary ratios at higher energy are needed, since it is here that the models begin to seriously diverge. Such future missions as ACCESS would be very helpful in determining which pictures of Galactic cosmic-ray propagation are feasible and which are not.

The authors are grateful to S. A. Stephens and R. A. Streitmatter for providing a database of cosmic-ray composition and energy spectra. We thank Toru Shibata for giving us updated sub-Fe/Fe ratios. This work was supported by NASA grant NAG5-7069.

REFERENCES

Aglietta, M., et al. 1993, Proc. 23d Int. Cosmic-Ray Conf. (Calgary), 2, 65
Alekseenko, V. V., et al. 1993, Proc. 23d Int. Cosmic-Ray Conf. (Calgary), 1, 483
Baring, M. G., Ellison, D. C., Reynolds, S. P., Grenier, I. A., & Goret, P. 1999, ApJ, 513, 311
Berezhko, E. G., & Ellison, D. C. 1999, ApJ, 526, 385
Berezinskii, V. S., Bulanov, S. V., Dogiel, V. A., Ginzburg, V. L., & Ptuskin, V. S. 1990, Astrophysics of Cosmic Rays (Amsterdam: North Holland)
Binns, W. R., Fickle, R. K., Waddington, C. J., Garrard, T. L., Stone, E. C., Israel, M. H., & Klarmann, J. 1981, ApJ, 247, L115
Chen, C.-X., et al. 1997, ApJ, 479, 504
Cutler, D. J., & Groom, D. E. 1991, ApJ, 376, 322
Davis, L., 1960, Proc. 6th Int. Cosmic-Ray Conf. (Moscow), 3, 220
Dorman, L. I., Ghosh, A., & Ptuskin, V. S. 1984, Astron. Lett., 10, 345
Esposito, J. A., Hunter, S. D., Kanbach, G., & Sreekumar, P. 1996, ApJ, 461, 820
Ferrière, K. 1998, ApJ, 497, 759
Ginzburg, V. L., Khazan, Y. M., & Ptuskin, V. S. 1980, Ap&SS, 68, 295
Ginzburg, V. L., & Ptuskin, V. S. 1976, Rev. Mod. Phys., 48, 161
Ginzburg, V. L., & Syrovatskii, S. I. 1964, The Origin of Cosmic Rays (Oxford: Pergamon)
Heinbach, U., & Simon, M. 1995, ApJ, 441, 209
Hillas, A. M. 1996, Proc. 24th Int. Cosmic-Ray Conf., Rapporteur Papers (Rome), 19C, 701
Jokipii, J. R. 1976, ApJ, 208, 900
Jones, F. C. 1979, ApJ, 229, 747
Lezniak, J. A., 1979, Ap&SS, 63, 279
Nagashima, K. K., et al. 1989, Nuovo Cimento, 12C, 695
Ptuskin, V. S. 1997, Adv. Space Res., 19, 697
Ptuskin, V. S., Jones, F. C., & Ormes, J. F. 1996, ApJ, 465, 972
Ptuskin, V. S., Jones, F. C., Ormes, J. F., & Soutoul, A. 1997, Proc. 25th Int. Cosmic-Ray Conf. (Durban), 4, 261
Ptuskin, V. S., Völk, H. J., Zirakashvili, V. N., & Breitschwerdt, D. 1997, A&A, 321, 434
Ruzmaikin, A. A., Sokolov, D. D., & Shukurov, A. U. 1988, Magnetic Fields of Galaxies (Dordrecht: Kluwer)
Seo, E. S., & Ptuskin, V. S. 1994, ApJ, 431, 705
Stephens, S. A., & Streitmatter, R. E. 1998, ApJ, 505, 266
Sturner, S. J., & Dermer, C. D. 1995, A&A, 293, L17
Webber, W. R. 1997, Space Sci. Rev., 81,107
Webber, W. R., Binns, W. R., Crary, D., & Westphall, M. 1994, ApJ, 429, 764
Webber, W. R., Kish, J. C, & Schrier, D. A. 1990, Phys. Rev. C, 41, 547
Webber, W. R., et al. 1998a, ApJ, 508, 940
———. 1998b, ApJ, 508, 949
———. 1998c, Phys. Rev. C, 58, 3539